Quantitative phase imaging using actively stabilized phase-shifting low-coherence interferometry

Hidenao Iwai,* Christopher Fang-Yen, Gabriel Popescu, Adam Wax,† Kamran Badizadegan, Ramachandra R. Dasari, and Michael S. Feld

G. R. Harrison Spectroscopy Laboratory, Massachusetts Institute of Technology, Cambridge, Massachusetts 02139

Received April 21, 2004

We describe a quantitative phase-imaging interferometer in which phase shifting and noise cancellation are performed by an active feedback loop using a reference laser. Depth gating via low-coherence light allows phase measurement from weakly reflecting biological samples. We demonstrate phase images from a test structure and living cells. © 2004 Optical Society of America

OCIS codes: 120.3180, 170.3880.

Optical coherence tomography (OCT) is an interferometric technique that produces depth-resolved images of backscattering from biological tissues.[1] OCT is generally concerned with measuring the envelope of the interference fringes rather than the phase of the backscattered light. Although the sensitivity of OCT is limited by the coherence length of the source to at best[2] approximately 1–2 μm, subnanometer pathlength changes can be detected through phase measurements.[3,4] Doppler OCT[5] and polarization OCT[6] make use of phase information to measure flow velocity and tissue birefringence, respectively. However, direct phase measurement in OCT is difficult because of phase noise in the interferometer from vibrations, air motion, thermal drifts, and other sources.

In this Letter we describe a method for producing a referenced phase measurement in which a reference laser beam is used to stabilize the interferometer, canceling interferometer noise through a piezoelectric feedback element. The present realization is a first step toward applying the principle in an OCT-type interferometer.

In our experiments, full-field images are obtained by phase-shifting interferometry, a standard technique often used for measuring surface topography.[7] High-resolution phase measurements by phase-shifting interferometry are typically possible only in mechanically stable environments, because of the high sensitivity of interferometers to external perturbations. A number of techniques for reducing phase noise[8] have been introduced, including methods using orthogonal polarizations,[9,10] high-speed imaging,[11] simultaneous imaging of several frames,[12] and active feedback cancellation of vibrations.[13] In an earlier study[14] a low-coherence interferometer with a harmonically related second wavelength as a phase reference was used to measure the phase of backscattered light from cultured cells and was sensitive to changes smaller than 10 nm.

This Letter presents a technique for using a reference laser beam to actively stabilize a Michelson–Linnik low-coherence interferometer. Active stabilization systems may be simpler and less expensive than high-speed or simultaneous imaging configurations and, unlike polarization schemes, can be used with highly birefringent samples. Use of a low-coherence light source allows measurement of phase profiles of surfaces with low reflectivity.

A schematic of the interferometer is shown in Fig. 1. A low-coherence beam from a superluminescent diode (EG&G SLD, central wavelength $\lambda = 845$ nm, FWHM bandwidth 20 nm) and a He–Ne laser beam ($\lambda_0 = 633$ nm) are combined by a dichroic beam splitter and enter an imaging interferometer similar to that described in Ref. 15. Achromatic lenses and aspheric objective lenses are arranged in a telescopic configuration with magnification $M = 19$. The reference mirror is mounted on a piezoelectric modulator (PZT). In the sample arm, objects of interest are aligned at the objective focus. Low-reflectivity samples are placed on a glass coverslip, the bottom of which is coated to be highly reflective at 633 nm but transmissive at 845 nm and the top of which is antireflection coated for light at 845 nm.

At the output of the interferometer, the two wavelengths are divided by a dichroic beam splitter. The 633-nm laser beam is detected by a photodiode and the 845-nm low-coherence beam by a CCD camera that

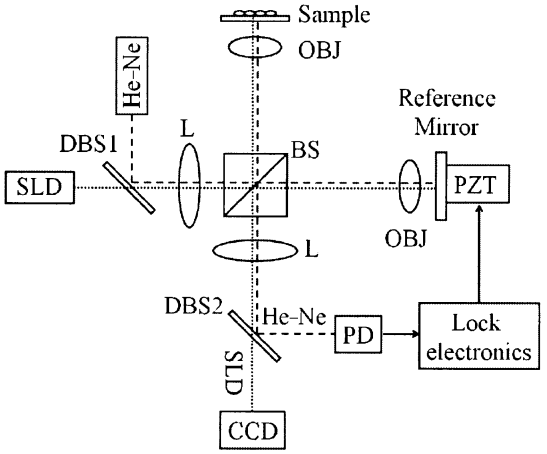

Fig. 1. Interferometer setup: SLDs, superluminescent diodes; He–Ne, helium–neon lasers; Ls, lenses; BS, beam splitter; OBJs, objective lenses; DBS1, DBS2, dichroic beam splitters. Dotted lines, beam path for the SLDs; dashed lines, beam path for the He–Ne.

0146-9592/04/202399-03$15.00/0

is aligned to produce a focused image of the sample under bright-field or dark-field microscopy. The reference-arm length is adjusted to produce interference at the CCD from the depth of interest in the sample arm. A variable neutral-density filter in the reference arm is varied to optimize fringe contrast.

To lock the interferometer, we developed a stabilization technique similar to that described in Ref. 16. The PZT is used both as a phase modulator and (at lower frequencies) to lock the interferometer and perform phase shifting. A feedback signal is created by sinusoidally modulating the PZT reference mirror at frequency $\Omega = 5$ kHz and amplitude of $\sim$20 nm. The photodiode signal is demodulated at the fundamental (Ω) and second-harmonic (2Ω) frequencies with lock-in amplifiers and is amplified to produce signals

$$V_1(t) = V_0 \sin[\phi_0 - \phi_{\mathrm{PZT}}(t) + \phi_N(t)], \quad (1)$$

$$V_2(t) = V_0 \cos[\phi_0 - \phi_{\mathrm{PZT}}(t) + \phi_N(t)], \quad (2)$$

where $\phi_0 = 2\pi(L_S - L_R)/\lambda_0$ is the round-trip phase difference between the sample and reference paths (not including phase noise or displacements from the PZT modulator), $\phi_{\mathrm{PZT}}(t) = 2\pi L_{\mathrm{PZT}}(t)/\lambda_0$ is the phase from the PZT modulator (not including the sinusoidal modulation), and $\phi_N(t)$ is the interferometer phase noise. Multiplying and summing electronics produces the linear combination

$$V_e(t) = \cos\theta V_1 - \sin\theta V_2 = V_0 \sin[\phi_0 - \phi_{\mathrm{PZT}}(t) + \phi_N(t) - \theta], \quad (3)$$

for some value of θ controlled by the computer. The signal $V_e(t)$ is then used as an error signal for an integrator circuit controlling the PZT voltage, which in turn controls $L_{\mathrm{PZT}}(t)$. Closing the loop drives the error signal to zero, giving $\phi_{\mathrm{PZT}}(t) = \phi_0 + \phi_N(t) - \theta$. In this way the PZT cancels interferometer noise and stabilizes the interferometer phase to an arbitrary angle θ.

Stabilization to arbitrary phase angles allows phase-shifting interferometry to be performed. Four CCD images $I_\theta(x, y)$ are recorded, with $\theta = 0, \pi/2, \pi, 3\pi/2$. From the four image frames the sample phase at each pixel is then calculated via

$$\phi(x,y) = \tan^{-1}\left\{\frac{[I_\pi(x,y) - I_0(x,y)]\sin(\pi r/2)}{[I_{\pi/2}(x,y) - I_{3\pi/2}(x,y)] - [I_\pi(x,y) - I_0(x,y)]\cos(\pi r/2)}\right\} - \frac{\pi}{2} r. \quad (4)$$

The factor $r = \lambda_0/\lambda$ compensates for the difference in wavelengths between locking and measurement beams.

Recording the four frames requires approximately 2 s, limited only by the CCD shutter speed and readout rate. Experimental control and data collection and analysis are performed with National Instruments LabVIEW software. For the data presented in this Letter phase unwrapping was not required.

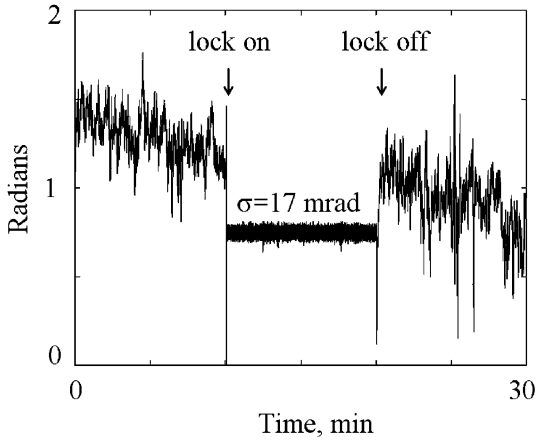

Fig. 2. Interferometer phase measurement of a test sample with a feedback loop open and closed (time 0–10 min and 20–30) and closed (time 10–20 min).

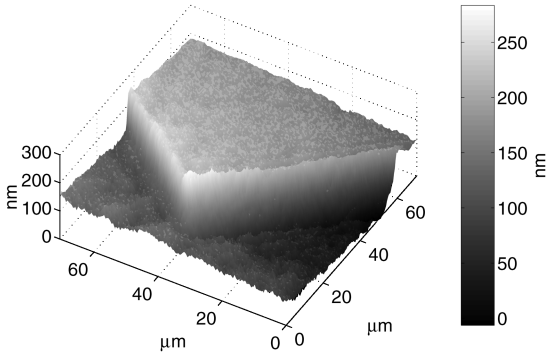

Fig. 3. Reflection phase image at the corner of a microfabricated silicon structure. The phase distribution is expressed as a surface height profile.

Figure 2 shows the error signal in the interferometer over a period of 30 min with a mirror as a test sample. The rms open-loop phase noise is approximately $\pi/5$, and a drift of $\sim$1 rad over the measurement time is present. On closure of the feedback loop, the standard deviation of the phase noise in the interferometer is reduced to $\sigma = 17$ mrad within the 8.3-Hz bandwidth of the system. This phase noise corresponds to an optical path length of 1.7 nm.

Using a mirror as a test object, we measured the noise of the stabilized phase-shifting interferometer for a single CCD pixel over 1 h. The standard deviation was found to correspond to an optical path length of approximately 6 nm, which can be reduced by CCD binning.

Figure 3 shows the phase profile of a portion of a microfabricated silicon structure measured in reflection. The height from the optical measurement of 139 $\pm$ 5 nm is consistent with a measurement of 150 $\pm$ 10 nm performed by an atomic force microscope. The relatively large error in the measurement may reflect nonuniformity of the sample.

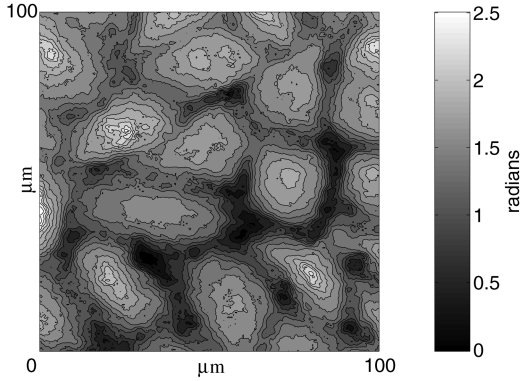

Fig. 4. Quantitative phase image of a confluent monolayer of HeLa cells.

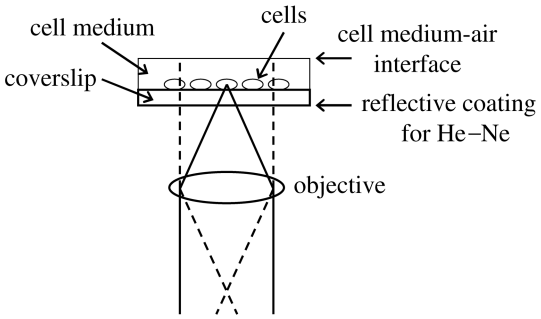

Fig. 5. Detail of the double-pass sample configuration for the image in Fig. 4. Dashed lines, illumination beam; solid lines, rays scattered from one point on the sample, showing the focus of the objective. The He–Ne locking beam is not shown.

For live cell imaging experiments, human epithelial cells (HeLa cells) were grown in chambered cover glasses at 37 °C in a culture medium. Figure 4 shows a phase image of a confluent monolayer of living cells obtained in a double-pass geometry (Fig. 5). The low-coherence light passes through the sample, reflects from a mirror or another reflective surface above the sample, and passes through the sample again. For these data the surface of the cell culture medium served as the reflective surface. The image of the cells from the initial pass is far out of focus, so variations in the measured phase distribution are determined only by the second pass. The transverse resolution of the imaging system is estimated to be 2 μm, limited by the 0.25 numerical aperture of the objective.

This transmission phase image is a measurement of optical path length differences between rays passing through different transverse points of the sample. Such quantitative measurement of the optical path can be used for determination of the dry weight of cells,[17] and the resulting phase images are useful for automated cell analysis.[18]

With further development this instrument will be used for imaging the phase of light directly backscattered from cells. In our current setup direct imaging of backscattering is difficult because of low fringe contrast and a limited dynamic range of our CCD camera. Reflection phase imaging of live cells will allow imaging of cellular motions on the nanometer scale, with potential applications in monitoring cell growth, activity, and volume regulation.

In summary, we have demonstrated a stabilized phase-shifting Michelson interferometer for phase imaging of reflected and transmitted light. Future studies will include quantitative investigation of subcellular structure and motions via transmitted and reflected light-phase imaging of cultured cells.

This research was conducted at the Massachusetts Institute of Technology Laser Biomedical Research Center and supported by the National Institutes of Health (P41-RR02594) and the Hamamatsu Corporation. C. Fang-Yen's e-mail address is minwah@mit.edu.

*Also with Hamamatsu Photonics K.K., Hamamatsu, Japan.

†Present address, Department of Biomedical Engineering, Duke University, Durham, North Carolina 27708.

References

1. D. Huang, E. A. Swanson, C. P. Lin, J. S. Schuman, W. G. Stinson, W. Chang, M. R. Hee, T. Flotte, K. Gregory, C. A. Puliafito, and J. G. Fujimoto, Science **254,** 1178 (1991).
2. W. Drexler, U. Morgner, F. X. Kärtner, C. Pitris, S. A. Boppart, X. D. Li, E. P. Ippen, and J. G. Fujimoto, Opt. Lett. **24,** 1221 (1999).
3. C. Yang, A. Wax, R. R. Dasari, and M. S. Feld, Opt. Lett. **27,** 77 (2002).
4. T. Akkin, D. P. Dave, T. E. Milner, and H. G. Rylander III, Proc. SPIE **4616,** 9 (2002).
5. Z. Chen, T. E. Milner, D. Dave, and J. S. Nelson, Opt. Lett. **22,** 64 (1997).
6. M. R. Hee, D. Huang, E. A. Swanson, and J. G. Fujimoto, J. Opt. Soc. Am. B **9,** 903 (1992).
7. K. Creath, in *Progress in Optics, Vol. XXVI*, E. Wolf, ed. (Elsevier, Amsterdam, 1998), pp. 349–393.
8. J. C. Wyant, Opt. Photon. News **14**(4), 36 (2003).
9. C. K. Hitzenberger and A. F. Fercher, Opt. Lett. **24,** 622 (1999).
10. D. P. Dave and T. E. Milner, Opt. Lett. **25,** 227 (2000).
11. A. Dubois, L. Vabre, A. C. Boccara, and E. Beaurepaire, Appl. Opt. **41,** 805 (2002).
12. C. L. Koliopoulos, Proc. SPIE **1531,** 119 (1992).
13. C. Zhao and J. H. Burge, Appl. Opt. **40,** 6215 (2001).
14. C. Yang, A. Wax, M. S. Hahn, K. Badizadegan, R. R. Dasari, and M. S. Feld, Opt. Lett. **26,** 1271 (2001).
15. L. Vabre, A. Dubois, and A. C. Boccara, Opt. Lett. **27,** 530 (2002).
16. A. A. Freschi and J. Frejlich, Opt. Lett. **20,** 635 (1995).
17. H. G. Davies and M. H. F. Wilkins, Nature **169,** 541 (1952).
18. D. Zicha and G. A. Dunn, J. Microsc. **179,** 11 (1995).